High-Efficiency Water-Transport Channels using the Synergistic Effect of a Hydrophilic Polymer and Graphene Oxide Laminates

Kang Huang, Gongping Liu, Jie Shen, Zhenyu Chu, Haoli Zhou, Xuehong Gu, Wanqin Jin, and Nanping Xu*

Graphene oxide (GO) laminates possess unprecedented fast water-transport channels. However, how to fully utilize these unique channels in order to maximize the separation properties of GO laminates remains a challenge. Here, a bio-inspired membrane that couples an ultrathin surface water-capturing polymeric layer (<10 nm) and GO laminates is designed. The proposed synergistic effect of highly enhanced water sorption from the polymeric layer and molecular channels from the GO laminates realizes fast and selective water transport through the integrated membrane. The prepared membrane exhibits highly selective water permeation with an excellent water flux of over 10 000 g m^{-2} h^{-1}, which exceeds the performance upper bound of state-of-the-art membranes for butanol dehydration. This bio-inspired strategy demonstrated here opens the door to explore fast and selective channels derived from 2D or 3D materials for highly efficient molecular separation.

1. Introduction

Recently, because of extraordinary physicochemical properties, nanosheets and nanolayers, such as zeolites and metal–organic frameworks, are seen as the future direction of membrane research by being used in mixed matrix[1–4] or stacked sheet membranes.[5,6] Among them, 2D nanostructured graphene oxide (GO) with extended lateral dimensions and nanometer thickness has become a promising candidate for membrane separations[7–10] because it can be easily stacked to form paper-like continuous membranes.[11,12] Up to now, many breakthroughs about GO membranes have been discovered and reported.[13–16] The exciting selective permeation results, including our recent studies,[17,18] have demonstrated that GO is a new-generation material platform for high-performance separation membranes with inspiring fast water,[18–21] gas,[14,15,17,22] and ion[23,24] transport channels. These intrinsic and unique channels offer a wide variety of applications for small-molecule separation under aqueous conditions[16,18–21,23,24] or for the separation of gas mixtures.[14,15,17,22] In addition, many simulation works also demonstrated that graphene-based membranes could show excellent separation performance in liquid or gas separation.[25–28]

However, there are still many challenges to the fabrication of GO laminates. GO laminates usually fail to achieve the theoretically predicted results in real separation processes. One reason may be that the *d*-spacing between GO layers is not constant and that it may vary according to different preparation methods.[29–31] Another reason may be that it changes easily under different feed environments.[32–34] Also, the formation of highly ordered, precise GO laminates through the self-assembly of GO nanosheets is extremely difficult.[35] Some inevitable nonselective defects or out-of-order accumulation will exist in the GO layers due to the repulsive electrostatic interactions caused by negatively charged carboxy groups.[14] Thus, the separation potential of GO laminates has not been fully explored. Despite these drawbacks, fully utilizing the unique channels of GO laminates could be a simple, feasible, and effective approach to optimizing the transport properties of GO laminates, which are expected to transcend the separation limitations of current state-of-the-art membranes.

How can we fully utilize the fast water, gas, or ion transport channels of GO laminates? There are phenomena in nature to be learned. One striking example is that of amphibians (e.g., frogs), whose skin is permeable to water.[36,37] In order to protect and compensate for their thin and delicate skin, frogs have evolved mucous glands principally distributed on their heads, backs, and tails to produce secretions. By collecting water from the humid environment, these secretions can effectively keep the frog's skin moist and maintain the frog's vital activities. This interesting phenomenon inspired us to fabricate a bio-inspired membrane coupling a surface water-capturing layer and GO laminates consisting of water channels. In this bio-inspired membrane, a hydrophilic polymer acts as the surface layer to preferentially capture a large number of water molecules from feed mixtures, resulting in an increase of the driving force across the GO laminates. Finally, the 2D water channels within the interlayers of GO nanosheets would be fully used, realizing fast and selective water permeation through the integrated

K. Huang, Dr. G. Liu, J. Shen, Dr. Z. Chu, Prof. H. Zhou, Prof. X. Gu, Prof. W. Jin, Prof. N. Xu
State Key Laboratory of Materials-Oriented Chemical Engineering
Nanjing Tech University
5 Xinmofan Road, Nanjing 210009, P. R. China
E-mail: wqjin@njtech.edu.cn

DOI: 10.1002/adfm.201502205

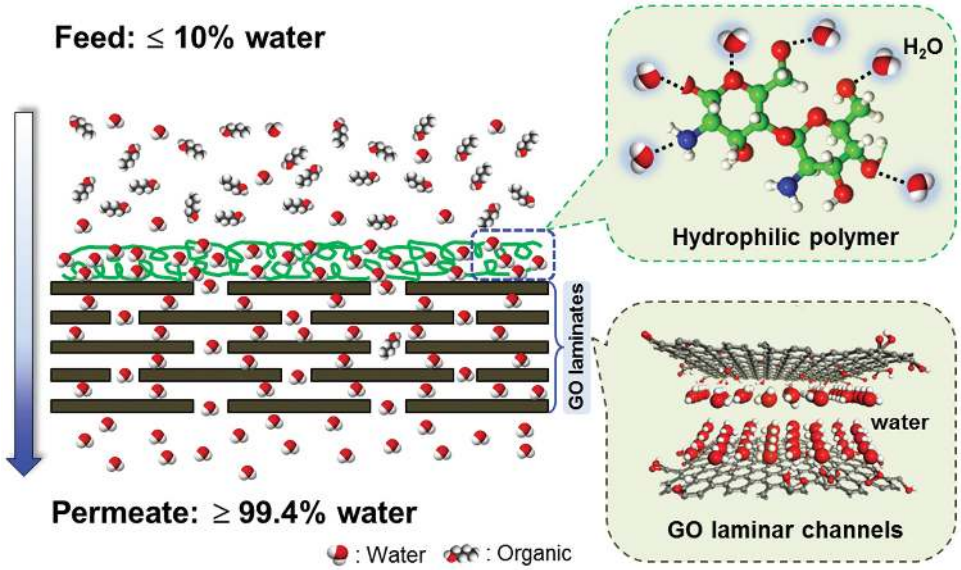

Figure 1. Schematic of the water–organic separation process using the synergistic effect of a hydrophilic polymer and GO laminates.

membrane. **Figure 1** is a schematic of the proposed separation process.

2. Results and Discussion

2.1. Membrane Morphologies

Herein, we used CS, an *N*-deacetylated derivative of chitin (a natural, inexpensive, and nontoxic *N*-acetyl-glucosamine polymer,[38] to fabricate the hydrophilic polymeric layer. The hydroxyl and amino groups in its repeat unit [see its structural diagram in Figure S1a (Supporting Information) and Fourier transform infrared (FTIR) spectra in Figure S1c (Supporting Information)] make it a highly hydrophilic material through the formation of hydrogen bonds with water molecules. First, we prepared the pristine GO laminates on α-Al_2O_3 ceramic hollow fiber supports, as previously described.[18] Then, the hydrophilic CS polymeric layer was fabricated on the pristine GO laminates by the vacuum suction method, which is described in detail in the Experimental Section. The final, as-prepared membrane is denoted as a CS@GO membrane. As shown in **Figure 2**a, the as-prepared CS@GO membrane is yellow, and there is no obvious difference in membrane color between the as-prepared membrane and the pristine GO laminates. Figure 2b shows that the surface morphology of the CS@GO membrane has many small, wave-like ripples and that it is smoother than the pristine GO laminates (Figure S2a, Supporting Information). This may be because the hydrophilic polymer fills in the low-lying "valleys" of the GO laminates. Field emission scanning electron microscope (FESEM) images taken after rotating both the pristine and the CS@GO samples 45°, which gives us a clearer perspective, are shown in Figure 2c and Figure S2b (Supporting Information), respectively. Atomic force microscopy (AFM) images (see **Figure 3**a, confirm that the average roughness (R_a) of the CS@GO membrane (≈52.24 nm) is less than that of the pristine GO laminates (≈61.05 nm), indicating that the CS polymer coated the surface of the GO laminates. In order to confirm the uniform distribution of the CS polymer on the surface of the GO laminates, we used energy-dispersive X-ray (EDX) spectroscopy to characterize the membrane surface. As shown in Figure 3b, nitrogen element is evenly distributed throughout the sample. In contrast, no nitrogen can be found on the pristine GO laminates. These results further prove that the CS polymer was uniformly attached to the GO laminates. The membrane is not only conducive to efficiently capture water molecules, but it also partially increases the membrane's mechanical stability in the event of physical damage.

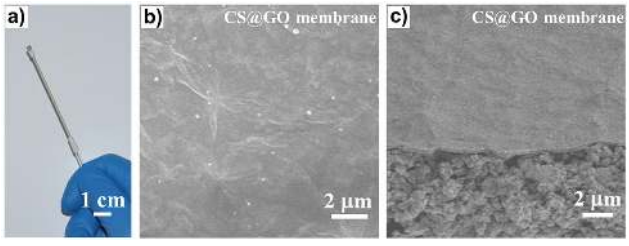

Figure 2. a) Digital photograph of the CS@GO membrane. b) Top-view FESEM image of the CS@GO membrane. c) FESEM image of the CS@GO membrane after rotating it 45°.

2.2. Membrane Microstructures

To the best of our knowledge, GO nanosheets bear many polar oxygenated functional groups [including hydroxyl, carbonyl, and carboxy groups; see its structural diagram in Figure S1b (Supporting Information) and FTIR spectra in Figure S1c (Supporting Information)].[39] These functional groups offer great potential for forming hydrogen and chemical bonds with the CS polymer, especially in the case of a high O/C ratio on GO (see X-ray photoelectron spectroscopy (XPS) spectra in Figure S3 in the Supporting Information). As shown in Figure 3c, after

Adv. Funct. Mater. **2015**,
DOI: 10.1002/adfm.201502205

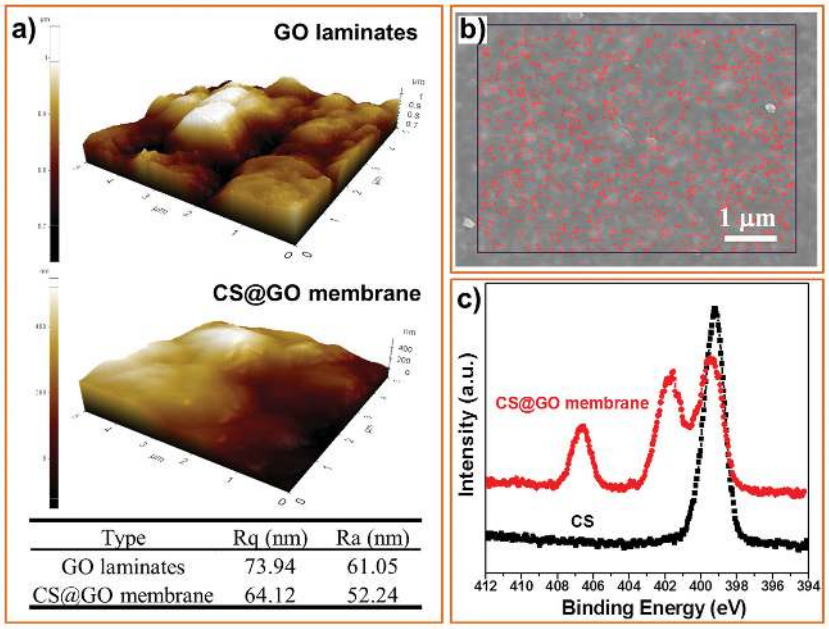

Type	Rq (nm)	Ra (nm)
GO laminates	73.94	61.05
CS@GO membrane	64.12	52.24

Figure 3. a) AFM images of the GO laminates and the CS@GO membrane and the corresponding root mean square roughness (R_q) and average roughness (R_a). b) EDX image of the surface of the CS@GO membrane (the red dots indicate the presence of N). c) XPS N1s spectra of the CS polymer and the CS@GO membrane.

coating the hydrophilic CS polymer onto the GO laminates, the N1s peaks shifted, indicating the intense interaction between GO and CS. This result was further confirmed by FTIR (Figure S4, Supporting Information). However, for the CS@GO membrane, a small Al2p peak, which exists in the GO layers, can be detected (Figure S5, Supporting Information). This Al in the GO layers originated from the α-Al_2O_3 hollow fiber support used in the preparation process.[40] The emergence of an Al peak shows that the thickness of the CS coating is less than 10 nm (the maximum probing depth of XPS in this work). This result is also close to our calculated value based on the CS density. The ultrathin CS coating, therefore, cannot be distinguished in the cross-sectional FESEM images of the CS@GO membranes (Figure S6, Supporting Information).

2.3. Permeation Properties

The separation performance of the CS@GO membrane was studied by measuring the pervaporation (PV) dehydration for butanol, which is a good solvent and an important chemical feedstock.[41,42] Butanol is also a new kind of advanced biofuel, because compared to conventional fuels it is less volatile and flammable, has a higher energy content, and is less hazardous to handle.[43,44] As shown in **Figure 4**a, the separation factor of the CS@GO membrane obviously increased as compared to the pristine GO laminates. The separation factor of the CS@GO membrane was 2580 at 30 °C, which is approximately six times larger than that of the pristine GO laminates at the same temperature. Meanwhile, the flux remained at a desired high level. By further increasing the operation temperature, the flux increases dramatically and the separation factor shows a gentle decline. Using the Arrhenius equation,[45] the activation energy (E_a) of *n*-butanol and water through the membrane were calculated (Figure S7 and Table S1, Supporting Information). The results show that *n*-butanol (e.g., 32.27 kg mol^{-1} of CS@GO membrane) has a higher E_a than water (e.g., 21.49 kg mol^{-1} of CS@GO membrane), indicating that the mass fraction of *n*-butanol in the permeate increases more than that of water with increasing operation temperature. Therefore, a higher flux and lower separation factor were obtained at high temperature.

2.4. Role of the Hydrophilic Polymer

However, this brings us to another crucial question: could the improvement of dehydration separation performance be related to the elimination of defects in the pristine GO laminates via coating with the hydrophilic CS polymer? Thus, we conducted a test to measure the molecular sieving properties for H_2/N_2 mixtures of the membranes before and

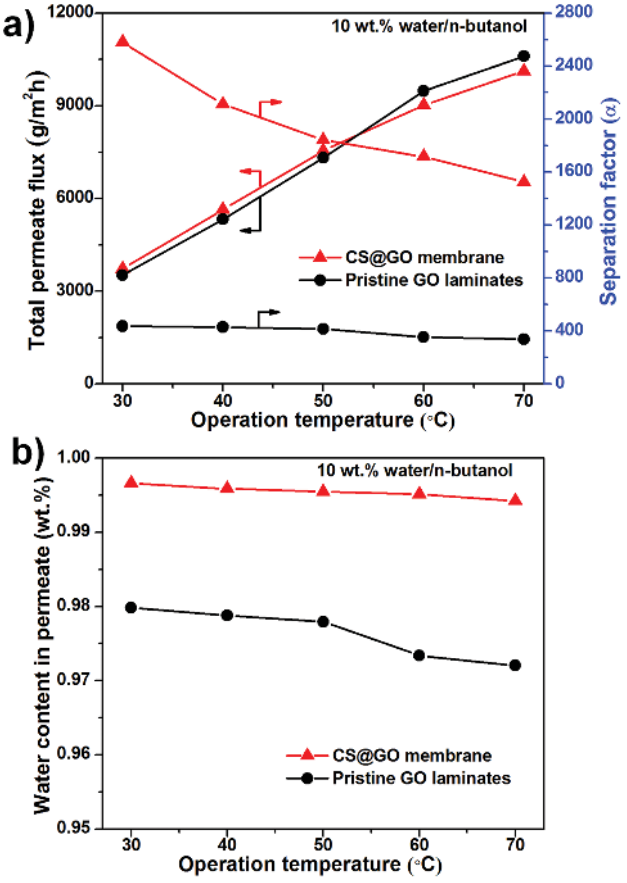

Figure 4. a) Flux and separation factor of the GO laminates and the CS@GO membrane for a 10 wt% water/*n*-butanol solution. b) The water concentration (wt%) in the permeate as a function of operation temperature.

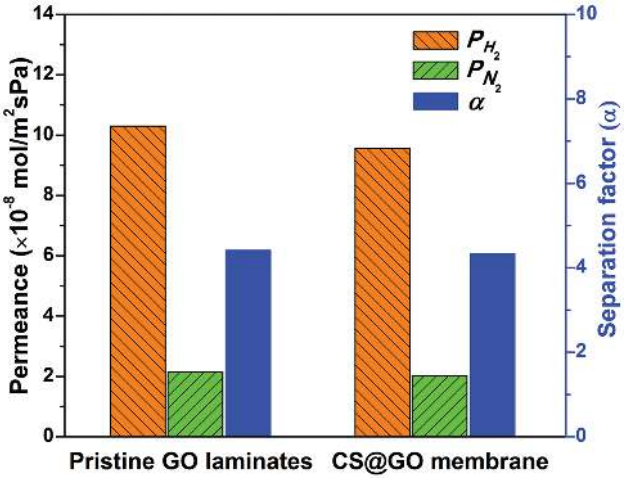

Figure 5. Gas separation performance of the GO laminates and the CS@GO membrane for a H_2/N_2 mixture (orange: the permeance of H_2; green: the permeance of N_2; blue: separation factor).

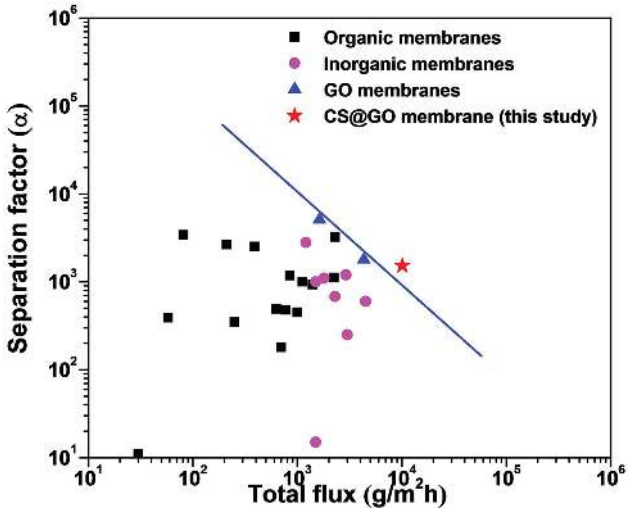

Figure 6. Comparison of GO membranes and the CS@GO membrane with state-of-the-art membranes for water/butanol dehydration. The detailed information is listed in Table S2 in the Supporting Information.

after CS coating. As shown in **Figure 5**, the H_2/N_2 separation factor does not change and agrees well with literature,[14] demonstrating that the vacuum-filtrated GO stacks are integrated and the introduced hydrophilic CS polymer captures water molecules on the surface of the GO laminates. The corresponding permeances of H_2 and N_2 declined slightly, which might be due to the additional mass transfer resistance of the polymeric layer. Therefore, it could be that the water penetration ability of the CS@GO membrane was enhanced because the hydrophilic CS polymeric layer captured more water molecules on the surface, as we proposed. At the same time, the permeation of *n*-butanol was suppressed. This caused an increase of the separation factor, whereas the additional mass transfer resistance of the CS layer balances the total flux of the GO laminates. By carefully comparing E_a before and after hydrophilic coating, one can find that E_a of the water for the CS@GO membrane becomes smaller than that for the pristine GO laminates (Table S1, Supporting Information). Whereas for *n*-butanol, it is reversed. This result means that water molecules can more easily pass through the CS@GO membrane, further proving that the water permeation ability of the GO laminates can be enhanced under the cooperative action of hydrophilic CS polymer and GO laminates.

Figure 4b shows the water concentration in the permeate as a function of operation temperature. In contrast to the pristine GO laminates, the permeate water concentrations of the CS@GO membrane are all above 99.4% across the whole range of testing temperatures (30–70 °C). This favorable temperature separation performance relationship further highlights the potential capability of the bio-inspired layer for capturing water on the surface. It is worth noting that at 70 °C, the permeation flux of the CS@GO membrane could exceed 10 000 g m^{-2} h^{-1} and simultaneously maintain a desired separation factor (1523). The excellent flux is more profitable for industrial applications because higher flux could significantly reduce the capital cost of membrane process. Compared to state-of-the-art membranes (including organic, inorganic and GO membranes), our membranes exhibit superior properties (see **Figure 6** and Table S2, Supporting Information).

2.5. Separation Mechanism

In order to further understand its separation mechanism, we conducted a series of experiments. The crystalline structure of the GO laminates was measured by X-ray diffraction (XRD) over the 2θ range of 3° to 15° in detail. As shown in Figure S8 (Supporting Information), the dry GO laminates show a diffraction peak at 2θ = 10.91°, corresponding to a GO *d*-spacing of 8.1 Å, which agrees well with the value reported by others.[13] After soaking the membrane in water, the GO laminates show a peak at 6.409°, which corresponds to a larger *d*-spacing of 13.7 Å. Therefore, the distance between GO layers is ≈10.2 Å (*d* = 13.7–3.5 Å. The thickness of a single GO layer is ≈3.5 Å), which is bigger than the diameter of *n*-butanol. These results mean that molecular sieving may not contribute significantly to the PV dehydration separation performance. In addition to molecular sieving, the hydrophilicity of GO also affects the performance. A preferential sorption–diffusivity mechanism was proposed in our previous work.[18] The preferential water-sorption ability and fast water diffusivity of the GO laminates mainly contribute to the dehydration. However, a consequent question is "which is the dominant factor?" Herein, we use the permeance to distinguish between the effect of operation conditions and that of the intrinsic properties of GO laminates on the PV performance.[46] The results show that with increasing operation temperature, the permeance of water decreases quickly from 168.3 to 62.4 mol m^{-2} h^{-1} kPa^{-1}, whereas that of butanol remains at ≈0.055 mol m^{-2} h^{-1} kPa^{-1}. Although the diffusivity could be enhanced by temperature, the sorption ability of the membranes would be weakened at higher temperature, leading to an overall decline in permeance. In other words, the water sorption process can be viewed as the control step in this case. For the CS@GO membrane, therefore, the hydrophilic polymeric layer, having an extraordinary adsorptive ability towards water molecules through strong hydrogen bonding, plays an important role in maximizing the selective water permeation property of GO laminates.

DOI: 10.1002/adfm.201502205

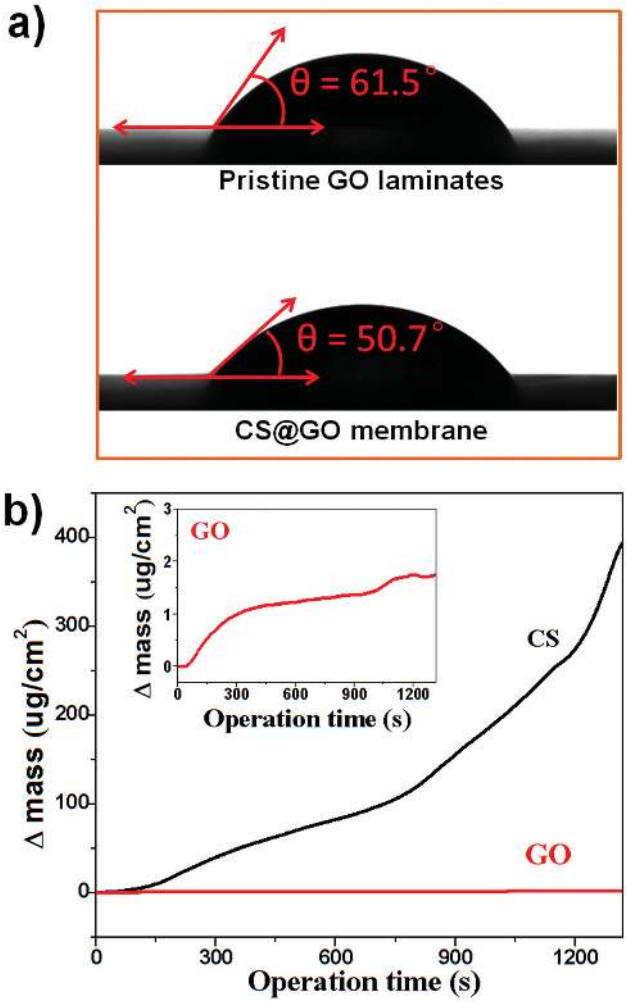

Figure 7. a) Contact angle of the pristine GO laminates and CS@GO membrane. b) Water-sorption ability of CS and GO measured by QCM. The inset is an enlarged figure for the water-sorption ability of GO.

To further identify the water-capture ability, we tested the water contact angle of the GO laminate surface before and after introducing the CS polymer. As shown in **Figure 7**a, the contact angle of CS@GO membrane decreases, indicating that the membrane becomes more hydrophilic. In addition, a quartz crystal microbalance (QCM) technique was carried out to compare the sorption ability of GO and CS. Figure 7b, shows that CS exhibits a much stronger water-sorption ability than GO. We also found that the mass of CS increased significantly when immersed in water. Similar phenomena were also found by other researchers.[47,48] Also, CS shows high water sorption selectivity for water/*n*-butanol mixtures (Figure S9, Supporting Information), which could also be beneficial for the dehydration process.

2.6. Synergistic Effect of CS and GO

In order to clarify the relationship between the individual and combined properties of CS and GO, we prepared pristine CS membranes on the same ceramic hollow fiber support for CS@GO membranes. As shown in Figure S10 (Supporting Information), the individual CS membrane did not exhibit high butanol dehydration performance, although the CS material owns strong water-sorption ability. Also, we fabricated sandwiched CS/GO/hollow fiber composite membranes by coating individual CS separation layer on the top of the pristine GO/hollow fiber membrane (see the SEM image in Figure S11a in the Supporting Information). However, both of the flux and separation factor (see Figure S11b in the Supporting Information) are much lower than that of the GO/hollow fiber membrane because of the increased mass transfer resistance. In addition, we incorporated GO nanosheets into the CS polymer matrix to prepare (CS + GO) hybrid membranes (so-called mixed matrix membranes, MMMs). Higher separation performance was not achieved too (see Figure S12 in the Supporting Information) because the disordered distribution of GO nanosheets cut off the promoted transport of water molecules (see Figure S13 in the Supporting Information). **Figure 8** gives a clear performance comparison of the pristine CS/hollow fiber membrane and GO/hollow fiber membrane, the sandwiched CS/GO/hollow fiber composite membrane, the (CS + GO)/hollow fiber hybrid membrane and the CS@GO/hollow fiber membrane.

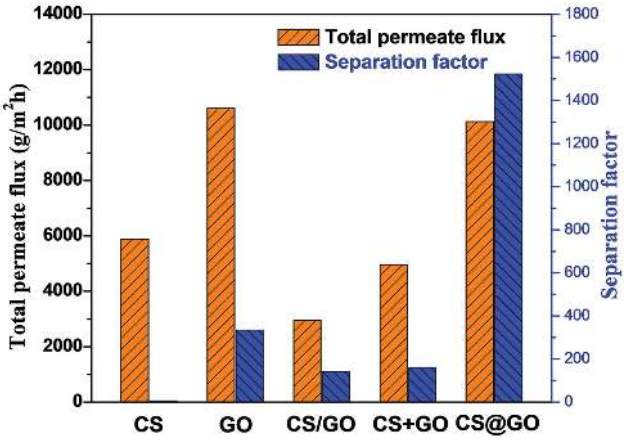

Figure 8. Performance comparison of the pristine CS/hollow fiber membrane and GO/hollow fiber membrane, the sandwiched CS/GO/hollow fiber membrane, the (CS + GO)/hollow fiber hybrid membrane and the CS@GO/hollow fiber membrane for 10 wt% water/butanol dehydration. These membranes are abbreviated as CS, GO, CS/GO, CS + GO, and CS@GO, respectively.

These above results confirmed us that highly fast-selective water permeation could not happen to the individual CS membrane or GO membrane. Moreover, it was verified that our observation of the high-performance CS@GO membrane cannot be accomplished by the simple combination of individual separation property of CS layer and GO laminates, whatever by "composite" or "hybrid" approach. As proposed in our work, the synergistic effect of highly enhanced water sorption from the polymeric layer and molecular channels from the GO laminates are believed to realize fast and selective water transport through the integrated membrane. By means of the elaborately designed CS@GO structure, water molecules captured by the ultrathin hydrophilic polymer could quickly transport through the fast water channels within the GO laminates (see Figure 1), high dehydration performance was thus achieved.

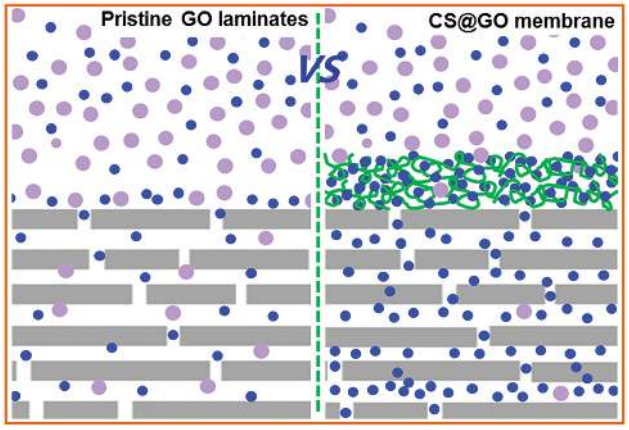

Figure 9. Schematic of the possible water–butanol separation process of GO laminates and the CS@GO membrane (water: blue solid circles; butanol: purple solid circles; GO nanosheets: gray sheets; hydrophilic polymer: green winding line).

However, in the pristine GO laminates, the fast water-transport channels were not fully utilized because of insufficient water molecules on the surface, as show in **Figure 9**.

2.7. Mechanical Stability

Could the hydrophilic polymeric layer decrease physical damage to the membrane by increasing its mechanical stability? To answer this question, we used a nanoscratch technology (**Figure 10**a) to assess the mechanical strength and interfacial adhesion of the membranes.[49] As shown in Figure 10b, the CS@GO membrane begins to fail with a drastic depth change at 233.7 mm, which is larger than that of the pristine GO laminates (141.6 mm, see Figure S14a in the Supporting Information). Substrate exposure also happened at these points. These transitions were confirmed by FESEM. As shown in Figure 10c, there are two clear different regions. At the second region, the larger cracking was formed on the membranes. The load-displacement curve [see Figure 10d and Figure S14b (Supporting Information)] reveals that the corresponding critical loads of the pristine GO and CS@GO membranes are 16.01 and 27.53 mN, respectively. These results demonstrate that the hydrophilic CS polymeric layer can not only enhance the water channels of GO laminates but also efficiently improve the mechanical stability of the membrane. Also, the enhanced interfacial adhesion further proves that the hydrophilic CS polymer is in close contact with the GO laminates.

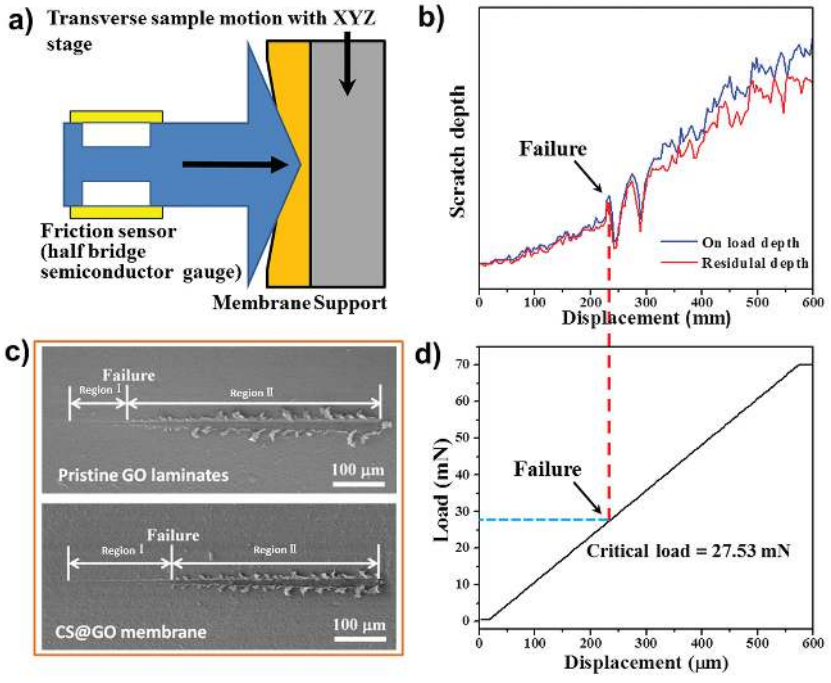

Figure 10. a) Schematic of the nanoscratch test. b) Scratch depth–displacement curve of the CS@GO membrane. c) FESEM images of the interfacial failure of the GO laminates and the CS@GO membranes. d) Load–displacement curve of the CS@GO membrane.

3. Conclusions

We demonstrated a novel bio-inspired strategy that utilizes the synergistic effect of a hydrophilic polymer and GO laminates to realize fast water-transport channels. By combining these materials, we constructed a high-efficiency membrane for water transport. The illustrated CS@GO membrane showed excellent water-selective permeation properties when separating low-water-content organic mixtures, which were attributed to the preferential water adsorption ability of the hydrophilic polymer together with the 2D water channels within the ordered GO laminates. Given the rapidly increasing interest in nanochannels for fast and selective transport, the concept and approach reported here would be a vital step toward realizing ultrafast and precise separation based on ordered 2D or 3D nanostructures.

4. Experimental Section

Preparation of the GO Laminates and CS@GO Membrane: A schematic of the fabrication steps is shown in Figure S15 (Supporting Information). First, the GO aqueous solution was prepared. Single-layered GO powder (Nanjing JCNANO Tech Co., Ltd, China) was prepared by modified Hummer's method. The GO powder was first dissolved into deionized water to make a high concentration GO aqueous solution (0.1 mg mL^{-1}). The resulting GO aqueous solution was treated ultrasonically for 30 min to exfoliate the GO to form GO nanosheets. Then, this GO aqueous solution was diluted 100 times to form a low-concentration GO aqueous solution (0.001 mg mL^{-1}). The GO laminates were fabricated on a ceramic hollow fiber support (Figure S16, Supporting Information) by the vacuum suction method previously reported.[18] The detailed processes are described as follows. One side of the ceramic hollow fiber was sealed and the other side was connected to a vacuum pump. Then, the whole support was immersed in the GO aqueous solution. Under the driving force of pressure, GO nanosheets were easily stacked on the surface of the support. In order to obtain a thin and continuous membrane layer, the time was

Adv. Funct. Mater. **2015**,
DOI: 10.1002/adfm.201502205

controlled to 0.5 h. Then, the as-prepared GO laminates were dried in a vacuum chamber at 45 °C for 48 h.

The CS@GO membrane was fabricated by a similar method. First, the CS polymer (>90% *N*-deacetylation degree, Sinopharm Chemical Reagent Co., Ltd, China) was dissolved into deionized water to form a 0.1 wt% CS aqueous solution. Then, the as-prepared GO laminates were immersed in the CS aqueous solution. The lumen of the hollow fiber was kept in vacuum and the time was controlled to 0.5 h. Finally, the as-prepared CS@GO membrane was dried in a vacuum chamber at 45 °C for 48 h.

Characterization: FTIR spectra were separately recorded using an FTIR spectrophotometer (AVATAR-FT-IR-360, Thermo Nicolet, USA) over the range of 4000–500 cm^{-1}. The XPS characterization was carried out through an X-ray photoelectron spectrometer (Thermo ESCALAB 250, USA) using monochromatized Al Kα radiation (1486.6 eV). The size of the GO nanosheets and the surface morphologies were obtained by AFM (XE-100, Park SYSTEMS, Korea) operated in the noncontact mode. The morphologies of the membranes and supports were examined via FESEM (S4800, Hitachi, Japan). The working parameters were a voltage (HV) of 5 kV and a work distance (WD) of 8 mm. With EDX spectroscopy, the working parameters were a voltage (HV) of 20 kV and a WD of 15 mm. The crystal phases of the samples were determined by XRD with Cu Kα radiation (Bruker, model D8 Advance). In order to precisely measure XRD patterns, a flat GO laminate sample was used. The contact angles of water were analyzed using a contact-angle Dropmeter (A100P, MAIST Vision Inspection and Measurement Co. Ltd). The quartz crystal microbalance technique (QCM200 Quartz Crystal Microbalance, Stanford Research Systems, Inc.) was used to test the sorption ability; the test was carried out as per our previous report.[18] Supplementary Notes 1–3 in the Supporting Information describe the detailed experiment about nanoscratch test, PV separation test, and gas separation test, respectively.

Supporting Information

Supporting Information is available from the Wiley Online Library or from the author.

Acknowledgements

K.H. and G.L. contributed equally to this work. This work was financially supported by the National Natural Science Foundation of China (Grant Nos. 21476107, 21490585, 21406107), the Innovative Research Team Program by the Ministry of Education of China (Grant No. IRT13070), a Project funded by the Priority Academic Program Development of Jiangsu Higher Education Institutions (PAPD) and the Innovation Project of Graduate Research by Jiangsu Province (Grant No. KYLX_0764).

Received: May 29, 2015
Revised: July 6, 2015
Published online:

[1] T. Rodenas, I. Luz, G. Prieto, B. Seoane, H. Miro, A. Corma, F. Kapteijn, F. X. Llabrés, I. Xamena, J. Gascon, *Nat. Mater.* **2015**, *14*, 48.
[2] H.-K. Jeong, W. Krych, H. Ramanan, S. Nair, E. Marand, M. Tsapatsis, *Chem. Mater.* **2004**, *16*, 3838.
[3] H.-K. Jeong, S. Nair, T. Vogt, L. C. Dickinson, M. Tsapatsis, *Nat. Mater.* **2003**, *2*, 53.
[4] E. L. Cussler, *J. Membr. Sci.* **1990**, *52*, 275.
[5] Y. Peng, Y. Li, Y. Ban, H. Jin, W. Jiao, X. Liu, W. Yang, *Science* **2014**, *346*, 1356.
[6] Z. P. Smith, B. D. Freeman, *Angew. Chem. Int. Ed.* **2014**, *53*, 10286.
[7] G. P. Liu, W. Q. Jin, N. P. Xu, *Chem. Soc. Rev.*, **2015**, *44*, 5016.
[8] H. Huang, Y. Ying, X. Peng, *J. Mater. Chem. A* **2014**, *2*, 13772.
[9] K. A. Mahmoud, B. Mansoor, A. Mansour, M. Khraisheh, *Desalination* **2015**, *356*, 208.
[10] T. Kim, J. H. Kang, S. J. Yang, S. J. Sung, Y. S. Kim, C. R. Park, *Energy Environ. Sci.* **2014**, *7*, 3403.
[11] Y. Su, V. G. Kravets, S. L. Wong, J. Waters, A. K. Geim, R. R. Nair, *Nat. Commun.* **2014**, *5*, 4843.
[12] L. Peng, Z. Xu, Z. Liu, Y. Wei, H. Sun, Z. Li, X. Zhao, C. Gao, *Nat. Commun.* **2015**, *6*, 5716.
[13] R. R. Nair, H. A. Wu, P. N. Jayaram, I. V. Grigorieva, A. K. Geim, *Science* **2012**, *335*, 442.
[14] H. W. Kim, H. W. Yoon, S. M. Yoon, B. M. Yoo, B. K. Ahn, Y. H. Cho, H. J. Shin, H. Yang, U. Paik, S. Kwon, J. Y. Choi, H. B. Park, *Science* **2013**, *342*, 91.
[15] H. Li, Z. Song, X. Zhang, Y. Huang, S. Li, Y. Mao, H. J. Ploehn, Y. Bao, M. Yu, *Science* **2013**, *342*, 95.
[16] W.-S. Hung, C.-H. Tsou, M. De Guzman, Q.-F. An, Y.-L. Liu, Y.-M. Zhang, C.-C. Hu, K.-R. Lee, J.-Y. Lai, *Chem. Mater.* **2014**, *26*, 2983.
[17] J. Shen, G. Liu, K. Huang, W. Jin, K. R. Lee, N. Xu, *Angew. Chem. Int. Ed.* **2015**, *54*, 578.
[18] K. Huang, G. Liu, Y. Lou, Z. Dong, J. Shen, W. Jin, *Angew. Chem. Int. Ed.* **2014**, *53*, 6929.
[19] H. Huang, Z. Song, N. Wei, L. Shi, Y. Mao, Y. Ying, L. Sun, Z. Xu, X. Peng, *Nat. Commun.* **2013**, *4*, 2979.
[20] Y. Han, Z. Xu, C. Gao, *Adv. Funct. Mater.* **2013**, *23*, 3693.
[21] M. Hu, B. Mi, *Environ. Sci. Technol.* **2013**, *47*, 3715.
[22] H. W. Kim, H. W. Yoon, B. M. Yoo, J. S. Park, K. L. Gleason, B. D. Freeman, H. B. Park, *Chem. Commun.* **2014**, *50*, 13563.
[23] R. K. Joshi, P. Carbone, F. C. Wang, V. G. Kravets, Y. Su, I. V. Grigorieva, H. A. Wu, A. K. Geim, R. R. Nair, *Science* **2014**, *343*, 752.
[24] P. Sun, M. Zhu, K. Wang, M. Zhong, J. Wei, D. Wu, Z. Xu, H. Zhu, *ACS Nano* **2013**, *7*, 428.
[25] J. Lee, N. R. Aluru, *J. Membr. Sci.* **2013**, *428*, 546.
[26] M. E. Suk, N. R. Aluru, *J. Phys. Chem. Lett.* **2010**, *1*, 1590.
[27] A. V. Titov, P. Král, R. Pearson, *ACS Nano* **2010**, *4*, 229.
[28] K. Sint, B. Wang, P. Král, *J. Am. Chem. Soc.* **2008**, *130*, 16448.
[29] Y. P. Tang, D. R. Paul, T. S. Chung, *J. Membr. Sci.* **2014**, *458*, 199.
[30] K. Goh, L. Setiawan, L. Wei, R. Si, A. G. Fane, R. Wang, Y. Chen, *J. Membr. Sci.* **2015**, *474*, 244.
[31] C.-H. Tsou, Q.-F. An, S.-C. Lo, M. De Guzman, W.-S. Hung, C.-C. Hu, K.-R. Lee, J.-Y. Lai, *J. Membr. Sci.* **2015**, *477*, 93.
[32] N. F. D. Aba, J. Y. Chong, B. Wang, C. Mattevi, K. Li, *J. Membr. Sci.* **2015**, *484*, 87.
[33] H. Huang, Y. Mao, Y. Ying, Y. Liu, L. Sun, X. Peng, *Chem. Commun.* **2013**, *49*, 5963.
[34] G. Li, L. Shi, G. Zeng, Y. Zhang, Y. Sun, *RSC Adv.* **2014**, *4*, 52012.
[35] W.-S. Hung, Q.-F. An, M. De Guzman, H.-Y. Lin, S.-H. Huang, W.-R. Liu, C.-C. Hu, K.-R. Lee, J.-Y. Lai, *Carbon* **2014**, *68*, 670.
[36] R. C. Toledo, C. Jared, *Comp. Biochem. Physiol. A* **1993**, *105*, 593.
[37] L. Goniakowska-Witalinska, U. Kubiczek, *Anat. Anz.* **1998**, *180*, 237.
[38] M. Rinaudo, *Prog. Polym. Sci.* **2006**, *31*, 603.
[39] D. R. Dreyer, S. Park, C. W. Bielawski, R. S. Ruoff, *Chem. Soc. Rev.* **2010**, *39*, 228.
[40] C.-N. Yeh, K. Raidongia, J. Shao, Q.-H. Yang, J. Huang, *Nat. Chem.* **2015**, *7*, 166.
[41] G. Liu, W. Wei, W. Jin, *ACS Sustainable Chem. Eng.* **2014**, *2*, 546.
[42] W.-D. Huang, Y. H. Percival Zhang, *Energy Environ. Sci.* **2011**, *4*, 784.
[43] X.-L. Liu, Y.-S. Li, G.-Q. Zhu, Y.-J. Ban, L.-Y. Xu, W.-S. Yang, *Angew. Chem. Int. Ed.* **2011**, *50*, 10636.
[44] B. Huang, Q. Liu, J. Caro, A. Huang, *J. Membr. Sci.*, **2014**, *455*, 200.
[45] X. Feng, R. Y. M. Huang, *J. Membr. Sci.* **1996**, *118*, 127.
[46] X. Feng, R. Y. M. Huang, *Ind. Eng. Chem. Res.* **1997**, *36*, 1048.
[47] S. Yong, M. Shrivastava, P. Srivastava, A. Kunhikrishnan, N. Bolan, *Reviews of Environmental Contamination and Toxicology*, *Vol. 233*, Springer, New York **2015**, p. 1.
[48] E. S. Dragan, *Chem. Eng. J.* **2014**, *243*, 572.
[49] W. Wei, S. Xia, G. Liu, X. Gu, W. Jin, N. Xu, *AIChE J.* **2009**, *56*, 1584.